Contents lists available at ScienceDirect

ISPRS Journal of Photogrammetry and Remote Sensing

journal homepage: www.elsevier.com

# Early assessment of crop yield from remotely sensed water stress and solar radiation data

Mauro E. Holzman[a,*], Facundo Carmona[a], Raúl Rivas[b], Raquel Niclòs[c]

[a] Instituto de Hidrología de Llanuras "Dr. Eduardo J. Usunoff", CONICET, UNCPBA-IHLLA, Azul-Tandil, Argentina
[b] Instituto de Hidrología de Llanuras "Dr. Eduardo J. Usunoff" (UNCPBA-CIC-MA), Comisión de Investigaciones Científicas de la provincia de Buenos Aires, Tandil B7000, Argentina
[c] Department of Earth Physics and Thermodynamics, University of Valencia, 46100 Burjassot, Spain

ARTICLE INFO

*Article history:*
Received 29 September 2017
Received in revised form 1 February 2018
Accepted 13 March 2018
Available online xxx

*Keywords:*
Food security
Yield estimation
Evapotranspiration
Crop water stress

ABSTRACT

Soil moisture (SM) available for evapotranspiration is crucial for food security, given the significant inter-annual yield variability of rainfed crops in large agricultural regions. Also, incoming solar radiation (Rs) influences the photosynthetic rate of vegetated surfaces and can affect productivity. The aim of this work is to evaluate the ability of crop water stress and Rs remotely sensed data to forecast yield at regional scale. Temperature Vegetation Dryness Index (TVDI) was computed as an indicator of crop water stress and soil moisture availability. TVDI during critical growth stage of crops was calculated from MODIS products: MODIS/AQUA 8-day composite LST at 1 km and 16-day composite vegetation index at 1 km. Rs data were obtained from Clouds and the Earth's Radiant Energy System (CERES). The relationship between TVDI, Rs and yield of wheat, corn and soybean was analyzed. High $R^2$ values (0.55–0.82, depending on crop and region) were found in different agro-climatic regions of Argentine Pampas. Validation results showed the suitability of the model RMSE = 330–1300 kg ha$^{-1}$, Relative Error = 13–34%. However, results were significantly improved considering the most important factor affecting yield. Rs proved to be important for winter crops in humid areas, where incoming radiation can be a limiting factor. In semi-arid regions, soils with low water retention capacity and summer crops, crop water stress showed the best results. Overall, results reflected that the proposed approach is suitable for crop yield forecasting at regional scale several weeks previous to harvest.



## 1. Introduction

It is expected that the world total population could reach 9.15 billion by 2050, which will impact on world agriculture (Alexandratos and Bruinsma, 2012; Global Harvest Initiative, 2014). In this context, it is crucial not only to increase agriculture production for food security and energy, but also to ensure environmentally sustainable systems. Also, growth in crop production will mainly come from yield increases rather than from arable land expansion and increases in cropping intensity. Thus, understanding the factors that affect crop yield should be important to face future crop production fluctuations due to global climate change, water demand and soil limitations.

Although world irrigated areas have been increasing in the last decades, cultivated areas are highly dominated by rainfed crops (Alexandratos and Bruinsma, 2012). In such systems, soil water availability is frequently the main factor for maintaining crop productivity (Holzman and Rivas, 2016; Tadesse et al., 2015). Soil moisture shows high spatial and temporal fluctuations caused by a wide range of factors like topography, rainfall, groundwater level and soil type. Remotely sensed information plays an important role in vegetation drought monitoring given the periodic coverage allowing continuous measurements at different scales. Thus, cost-effective systems that provide early warning risk reduction in crop productivity during extreme events (e.g. drought and water excess) are highly valuable.

Over the last years, different studies have investigated the relationship between crop indices (e.g. vegetation indices, leaf area index), soil moisture or evapotranspiration and crop yield (Anderson et al., 2016; Holzman et al., 2014a; Holzman and Rivas, 2016; Leroux et al., 2016; Mladenova et al., 2017; Wu et al., 2014). Overall, vegetation-related attributes and indices are based mainly on spectral reflectance properties as indicators of vegetation health, status and aboveground biomass (Mladenova et al., 2017). Soil moisture and evapotranspiration methods are based mainly on temperature/energy balance approaches, estimating land surface temperature (LST) from thermal infrared (Mallick et al., 2009; Wagle et al., 2017) or microwave bands (Liu et al., 2017). Hence, LST is used as a proxy of latent heat flux and root zone soil water availability (Holzman et al., 2014b; Rivas and Caselles, 2004).

Thermal/reflectance remote sensing methods have been proved to be effective in detecting drought and vegetation production. Wu et al. (2014) evaluated a model based on enhanced vegetation index (EVI), LST from MODIS and radiation data from the National Center for Environmental Prediction (NCEP). That model provided better results of gross primary production (GPP) than the standard MODIS GPP product for forest and non-forest areas. In Brazil, Anderson et al. (2016) found strong correlations between corn, soybean and cot-

* Corresponding author at: IHLLA, Rep. Italia 780, Azul B7300, Argentina.
*Email address:* mauroh@faa.unicen.edu.ar (M.E. Holzman)

https://doi.org/10.1016/j.isprsjprs.2018.03.014
0924-2716/ 

ton yield and the Evaporative Stress Index computed from LST and leaf area index (LAI) data from MODIS. In the Sahelian region, Leroux et al. (2016) reported correlation (r = 0.59) between LST and NDVI from MODIS and simulated pearl millet. Also, Mladenova et al. (2017) showed that evapotranspiration and soil moisture indices can provide better information for estimating corn and soybean yields than vegetation indices, given the conservative characteristic of those indices as indicators of water stress. In Holzman et al. (2014a), Holzman and Rivas (2016) we analyzed the capability of the Temperature Vegetation Dryness Index (TVDI) computed from LST and EVI from MODIS to estimate wheat, soybean and corn yield in the Argentine Pampas. Results showed that TVDI during the critical growth stage is a suitable indicator of crop water stress and the impact on crop yield at regional scale ($R^2 \geq 0.70$). Also, in Argentina Sayago et al. (2017) compared the TVDI from Landsat with indicators of soybean water stress.

Although these studies have proven the extensive analysis of thermal and reflectance data as crop water stress indicators, it should be noted that solar radiation could be a limiting factor for crop production in areas with persistent cloud cover (e.g. humid and sub-humid regions). Solar radiation influences the photosynthetically active radiation absorbed by canopy and then, vegetation production (Monteith, 1977). In addition, Xin et al. (2016) concluded that the partitioning of diffuse and direct solar radiation should be considered for modeling production on a daily or shorter basis. Argentina is one of the main grain exporters, especially corn, wheat and soybean (Argentina is the third producer of soybean with 40–56 million tonnes per year), and the production comes mainly from the Argentine Pampas. The works carried out in this region have been focused mainly on crop water stress and the limiting effect of incoming solar radiation still needs to be addressed. The aim of this work is to evaluate the combination of a soil water availability indicator through TVDI and incoming solar radiation to estimate spatially corn, wheat and soybean yield prior to harvest in the Argentine Pampas. Thus, this study shows a novel approach that also considers the effect of solar radiation on crop yield.

## 2. Background

Thermal remote sensing methods that can provide estimates of water status in soil-plant system are based on principles of energy conservation through the surface energy balance equation:

$$Rn = LE + H + G \quad (1)$$

where Rn is the net radiation, LE is the latent heat flux (evapotranspiration), H is the sensible heat flux and G is the soil heat flux ($G \approx 0$ over maximum vegetation cover). The H and LE terms are difficult to calculate from remotely sensed data and can be estimated using models of different complexity (Wagle et al., 2017). However, LST has been widely used as an indicator of H. The incoming solar radiation (Rs) is the main radiative variable determining the Rn and LE. Aerodynamic effects influence LE and H. Over vegetated areas, with a given available energy incident at surface (Rn-G), the distribution of solar radiation into H and LE depends mainly on stomatal resistance to respiration (Holzman and Rivas, 2016; Rivas and Caselles, 2004). Such stomatal resistance is strongly influenced by root zone soil water availability (Kurc and Small, 2004), and determines the coupled water and carbon fluxes with the atmosphere. Thus, LST is a simple proxy of root zone soil water availability and the impact of these conditions on crop productivity (Bhattacharya et al., 2011; Holzman et al., 2014a). On the other hand, vegetation indices reflect the amount of vegetation and the photosynthetic capacity. They have been widely applied to monitor vegetation water stress, although they reflect drought effects in advanced stage (Farquhar and Sharkey, 1982).

In Holzman et al. (2014a), Holzman and Rivas (2016) a model to estimate crop water stress and yield was evaluated in the Argentine Pampas. The model considers only limitations to yield due to soil water availability:

$$Y_r = C_1(TVDI_{cum})^2 + C_2(TVDI_{cum}) + C_3 \quad (2)$$

where $Y_r$ is the actual crop yield, $TVDI_{cum}$ is the cumulative TVDI during crop critical growth stage, $C_1$, $C_2$ and $C_3$ are coefficients of regression between TVDI and yield depending on agro-climatic regions (Holzman and Rivas, 2016). TVDI is based on the negative correlation between LST and EVI (Sandholt et al., 2002):

$$TVDI = \frac{LST - LST_{\min}}{LST_{\max} - LST_{\min}} \quad (3)$$

where LST is the observed surface temperature at a given pixel, $LST_{min}$ is the minimum temperature (maximum LE) for a certain region. $LST_{max}$ is the maximum temperature for a given EVI in the LST/EVI scatterplot of a region, calculated as a linear fit to EVI ($LST_{max} = aEVI + b$). The a and b parameters are the intercept and slope of linear adjustment of $LST_{max}$. This index takes values between 0 and 1 indicating maximum and minimum soil water availability, respectively.

The TVDI is based on the LST/vegetation index (VI) triangular space (Sandholt et al., 2002), which has been used in several works to monitor vegetation water stress (e.g. Holzman and Rivas, 2016; Nutini et al., 2014). Meteorological data are not required for its calculation, although it is an integrative index that takes into account the main surface-atmosphere processes of the surface energy balance and the photosynthetic rate of vegetated areas. Fractional vegetation cover, sensed through VI, determines the amount of vegetation visible to the sensor, which will affect the spatially integrated LST. Evapotranspiration mainly determines the LST through the energy balance of the surface. Incident radiation is one of the main drivers of LST and also affects the stomatal resistance to transpiration (Sandholt et al., 2002). Atmospheric forcing controls the flux of heat from surface to the atmosphere, and hence, the LST. Also, surface roughness and mixing level influence the heat conductivity into the atmosphere and the LST/VI space (Nemani and Running, 1997). In spite of the multiple interacting processes, root zone soil moisture is a key variable determining crop water stress and the mechanisms involved.

However, possible error sources in estimation of TVDI should be considered:

(1) $LST_{max}$ should be obtained taking into account pixels with minimum (theoretically, zero) evapotranspiration (transpiration from vegetation and evaporation from bare soil), with LST reaching a physical maximum when no evaporative cooling occurs. Conversely, $LST_{min}$ should reflect potential evapotranspiration over vegetated surfaces, where maximum evaporative cooling occurs. These model parameters have to be estimated on the basis of LST/VI space of a region with uniform atmospheric forcing. Otherwise, the sensitivity of the method decreases and it is not useful to detect crop water scarcity.

(2) The triangular shape is evident if different conditions of fractional vegetation and soil moisture are taken into account and if medium resolution images are used (e.g. 250 m–1 km). Otherwise, the $LST_{max}$ and $LST_{min}$ can be underestimated and overesti-

mated, respectively. On the other hand, these resolutions allow considering large areas and hence, the probability of local parameterization is minimized.

(3) Cloud cover restricts the calculation of TVDI because of fluctuations in net radiation or the lack of data.

Using this model we found a significant yield loss (wheat, soybean and corn) in the Argentine Pampas. Also, yield loss due to water excess was evident, although this point needs more analysis than has currently been done.

Given that evapotranspiration largely controls crop productivity, a more generalized model that considers water deficit and excess can be proposed:

$$Y_r = f\left(ET_a\right) = f\left(SM.ET_p\right) \tag{4}$$

where SM is a factor that considers root zone soil moisture. $ET_p$ is mainly controlled by the available energy (Bhattacharya et al., 2011; Stisen et al., 2008) and represents the radiative factor. Thus, $ET_p$ is proportional to Rs:

$$ET_p \propto \frac{Rs_a}{Rs_{\max}} \tag{5}$$

where $Rs_a$ is the incoming solar radiation at surface in all-sky conditions and $Rs_{max}$ is the theoretical incoming clear-sky solar radiation (Carmona et al., 2014, 2017).

In Holzman et al. (2014b) we showed that TVDI is suitable to evaluate root zone soil moisture over cultivated areas, whereby SM factor can be expressed in function of such index. Thus, considering Eqs. (4) and (5), a new approach considering yield loss due to limited soil water and incoming solar radiation can be expressed as:

$$\begin{aligned} Y_r &= f\left[(TVDI)\left(\frac{Rs_a}{Rs_{\max}}\right)\right] \\ &= f\left[(TVDI)\,(1-CC)_{cum}\right] \end{aligned} \tag{6}$$

where CC expresses the attenuation of solar radiation due to cloud cover. To obtain yield estimates (e.g. kg ha$^{-1}$), this model should be calibrated analyzing the relationship between TVDI, CC and field data of yield at regional or landscape scales during normal, humid and dry periods. This model considers the coupled effect of water availability and Rs on the final crop yield. The amount of absorbed solar radiation determines the amount of energy available and crop growth rate and, also influences the atmospheric evaporative demand. On the other hand, water scarcity (and consequently high TVDI) influences the water and carbon fluxes with the atmosphere. This condition may shorten the growing period determining the effective amount of radiation captured by the crop, which in turn reduces the final yield. In addition, water excess may be associated with waterlogging, reduced drainage, reduction of total root and canopy development (low intercepted solar radiation).

## 3. Study area and data sets

### 3.1. Agro-climatic regions

The Argentine Pampas is a large plain (with slopes of less than 1%) covering more than 50 million hectares of land suitable for crop production and livestock raising and is characterized by a subhumid temperate climate. Argiudoll is the main soil great group with organic matter content of the A horizon varying approximately between 2% and 5% (Holzman et al., 2017). The land cover of this region corresponds mainly to rainfed crops and a mosaic of cropland and vegetation (grassland, shrubland, forest) (Arino et al., 2008). Cultivated areas are highly dominated by rainfed crops, being soybean, corn and wheat the most important. Rainfall decreases from the eastern humid to the western semi-arid areas. Also, the interannual variability determines occasional droughts and floods, producing noticeable crop yield fluctuations (Holzman et al., 2014a). The joint assessment of SM and radiative factors to estimate crop yield was carried out in four agro-climatic regions (Fig. 1 and Table 1). Together with Northern Hills, Endorreic Pampas is the most productive region, given the high organic matter content of soils (≈3.5–5%) and abundant rainfall (occasional water deficit occurs during summer months and water excess during winter and autumn, overall in Northern hills). Also, Northern Hills is characterized by soils with high water retention capacity. On the other hand, Sandy Pampas has sporadic limitations for

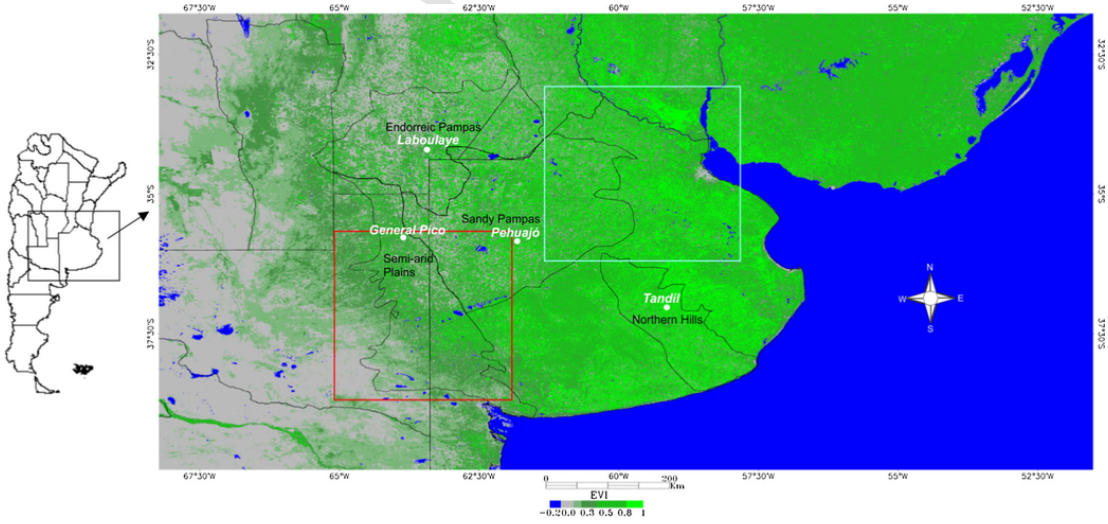


**Fig. 1.** The study area, the four analyzed agro-climatic regions of Argentine Pampas and meteorological stations. Rectangles show the areas used for $LST_{min}$ and $LST_{max}$ calculation (EVI image, October 2010).

**Table 1**
Characterization of the four analyzed regions.

| Agro-climatic zones | Dominant soil type | Mean annual temperature | Main crop (summer/winter) | R/ETp April–Sep[a] | R/ETp Oct–March[a] | R/ETp Annual[a] |
|---|---|---|---|---|---|---|
| Endorreic Pampas | Hapludoll and Haplustol | 18 °C | Soybean/wheat | 0.60 | 0.80 | 0.75 |
| Sandy Pampas | Udipsament | 18 °C | Soybean/wheat | 0.93 | 0.85 | 0.87 |
| Northern Hills | Typic Argiudoll | 16 °C | Soybean/wheat | 1.32 | 0.83 | 0.96 |
| Semi-arid Plains | Haplustoll | 20 °C | Sunflower/wheat | 0.69 | 0.81 | 0.78 |

[a] R/ETp = rainfall (mm)/potential evapotranspiration (mm). Meteorological stations considered for the analysis: Endorreic Pampas: Laboulaye (63°22′W; 34°08′S); Sandy Pampas: Pehuajó (61°54′W; 35°52′S); Northern Hills: Tandil (59°14′W; 37°15′S); Semi-arid Plains: General Pico (63°45′W; 35°42′S). Period: 1970–2013 (data source: Servicio Meteorológico Nacional and Ministerio de Agroindustria).

crops due to low water retention capacity. In semi-arid Plains crop yield reduction is common due to water deficit (December-February).

### *3.2. Satellite data*

The SM factor of Eq. (4) was estimated as a function of monthly TVDI. TVDI was calculated for the critical growth stage and dominant crops in each region using LST and EVI data from MODIS/AQUA. For each month, four 8-day composite LST, version 5, 1 km spatial resolution (MYD11A25) and two 16-day composite vegetation indices, version 5, 1 km spatial resolution (MYD13A25) were averaged. In terms of the spatial resolution, in Holzman and Rivas (2016) we found that 1 km is suitable to monitor crops in most of Argentine Pampas, given the dominant monoculture with plot size ≈ 100 has. AQUA data were used to consider the period of maximum atmospheric evaporative demand during the day (2:00–3:00 PM). Thus, changes in LST should be mainly caused by soil water availability. Five campaigns were considered to include different soil water and climatic conditions: drought (2007–2008), normal (2009–2010, 2010–2011, 2014–2015), and humid (2002–2003).

TVDI is based on semi-empirical interpretation of the LST and vegetation indices relationship. It was obtained defining $LST_{max}$ and $LST_{min}$ from the LST-EVI monthly triangular space (Fig. 2). As stated in previous works (Holzman et al., 2014a; Mallick et al., 2009; Sandholt et al., 2002), a wide range of soil water and vegetation cover conditions is needed to determine the TVDI parameters. $LST_{max}$ was obtained in semi-arid region to ensure that this edge reflects minimum soil moisture and evapotranspiration (Fig. 1). "a" and "b" parameters of $LST_{max}$ were estimated using the method of least squares (significance level of 5%) extracting points with maximum LST for different EVI intervals. To avoid the seasonal influence on these parameters, the extreme $LST_{max}$ (maximum slope and intercept) was defined comparing monthly "a" and "b" parameters (Fig. 2). Thus, this observed edge is as closest as possible to the theoretical dry edge that shows complete stomatal closure, zero water availability and evapotranspiration (Stisen et al., 2008). $LST_{min}$ was calculated from LST-EVI scatterplot of humid area and was considered as a horizontal line parallel to the EVI axis by averaging points with minimum LST for different EVI values. The minimum monthly $LST_{min}$ was considered as the extreme edge representing potential evapotranspiration (Fig. 2). Finally, comparable monthly TVDI was calculated using these extreme edges.

The radiative factor of Eq. (5) was estimated from the "CERES" (Clouds and the Earth's Radiant Energy System) data, which are satellite instruments of the NASA's Earth Observing System (EOS) that measure both solar-reflected and Earth-emitted radiation from the top of the atmosphere (TOA) to the Earth's surface. These data are combined with multiple source data (e.g. MODIS, VIIRS and geostationary satellites) to generate different products, including surface fluxes. The CERES instrument provides sampling at four local times: 0130, 1030, 1330, and 2230 at the Equator. This information can be computed at daily and monthly scales. Monthly Ed3A of

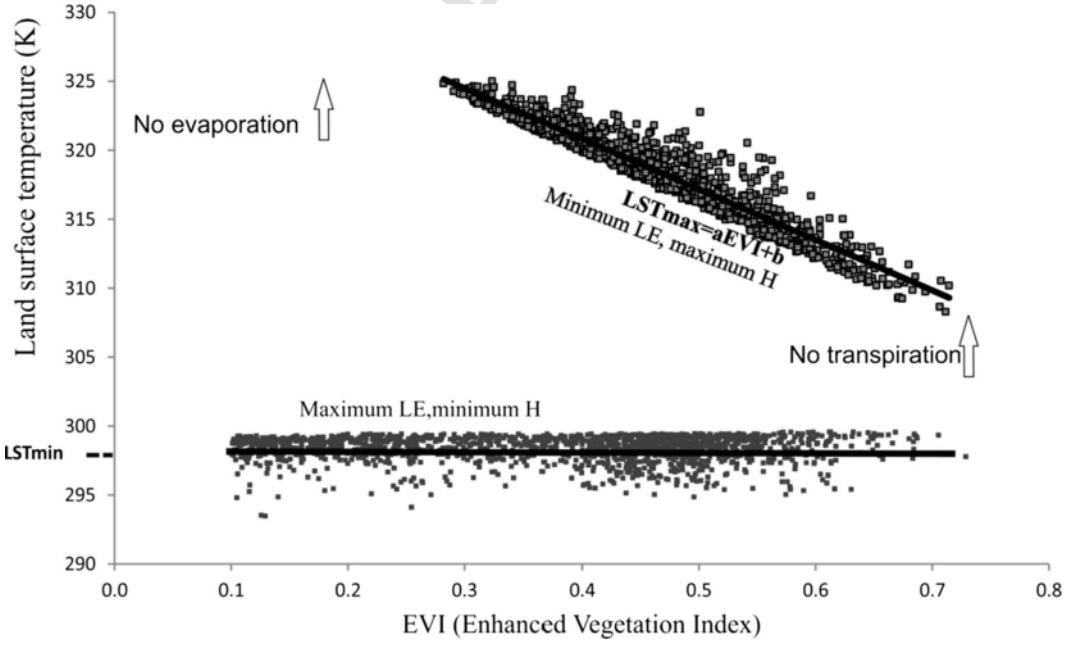


**Fig. 2.** Scheme of triangular LST/EVI scatter plot. Extreme $LST_{min}$ (maximum evapotranspiration) and $LST_{max}$ (minimum evapotranspiration) used to compute TVDI are included.

CERES_SYN1deg product data were used (http://ceres.larc.nasa.gov/), which provides downward shortwave radiation data on clear ($Rs_{max}$ of Eq. (5)) and all sky ($Rs_a$ of Eq. (5)) conditions (Synoptic Radiative Fluxes and Clouds) at 1 degree lat/long spatial resolution (Smith et al., 2011). Finally, CC (Eq. (6)) was estimated as a function of downward shortwave radiation on clear and all sky conditions.

### 3.3. Crop yield data

Official statistics of crop yield (kg ha$^{-1}$) in Argentina are available at county level. For each season of the study period, yield data of wheat, soybean and corn were extracted. Given that soil and climate type affect crop yield (Holzapfel et al., 2009; Holzman and Rivas, 2016), regression adjustments between remotely sensed data and yield of dominant crops were analyzed in each agro-climatic region. Table 2 shows the analyzed counties. Based on EVI images of MODIS/AQUA 16-day composite EVI at 250 m spatial resolution (MYD13Q1), nonagricultural lands were removed (water bodies and natural grassland) from the analysis. The cultivated pixels were averaged to produce estimates of TVDI at county level.

Several authors reported that crop status during critical growth stage (generally flowering, heading, milking or grain filling) is decisive to estimate yield prior to harvest (Anderson et al., 2016; Bhattacharya et al., 2011; Holzman et al., 2014a; Mkhabela et al., 2005). Also, that stage coincides with maximum vegetation cover and hence, minimum background effect of soil on TVDI. In this stage TVDI signal comes mainly from vegetation transpiration and photosynthetic rate. Based on studies of the crops phenology, (Oficina de Riesgo Agropecuario-MAGyP-Argentina, 2017) stated that this stage can comprise from October to February, depending on crop and region. Considering the dataset used in the TVDI-Rs-yield adjustments, a comparison between monthly TVDI-Rs and yields of each crop was carried out to define more precisely the critical growth months. Thus, the months with the highest coefficient of determination in each agro-climatic region were selected as critical stage (Holzman and Rivas, 2016). Then, yield data (dates or counties not used in the adjustments) were compared with yield estimated by the model to validate the ability of the TVDI-Rs model to estimate crop yield (Table 2). Validation parameters were: root mean square error (RMSE), relative error to average yield (RE) and index of agreement d (Willmot, 1981).

**Table 2**
Counties evaluated for crop yield adjustments (A) and validation (V).

| Agro-climatic region | County | Central coordinates (lat/long) | Total area (km$^2$) | Cultivated area (%) |
|---|---|---|---|---|
| Endorreic Pampas | General Roca (A) | 64°20′W; 34°33′S | 14,890 | 77 |
| | General Villegas (A, V) | 62°58′W; 34°47′S | 7345 | 84 |
| | General López (A, V) | 61°47′W; 33°49′S | 15,950 | 87 |
| | Roque Saenz Peña (A, V) | 63°22′W; 33°58′S | 9418 | 82 |
| | Juárez Celman (V) | 63°32′W; 33°09′S | 7630 | 96 |
| Sandy Pampas | Carlos Casares (A) | 61°20′W; 35°45′S | 2540 | 85 |
| | Carlos Tejedor (A) | 62°25′W; 35°22′S | 3919 | 68 |
| | Pellegrini (A) | 63°13′W; 36°15′S | 1885 | 88 |
| | General Viamonte (A, V) | 61°01′W; 34°59′S | 2160 | 88 |
| | 25 de Mayo (A, V) | 60°14′W; 35°29′S | 4780 | 85 |
| | Tres Lomas (A, V) | 62°51′W; 36°29′S | 1260 | 95 |
| | General Arenales (V) | 60°41′W; 34°18′S | 1476 | 80 |
| | Lincoln (V) | 61°42′W; 35°03′S | 5760 | 91 |
| | Pehuajó (V) | 61°57′W; 35°53′S | 4570 | 71 |
| | Rivadavia (V) | 63°06′W; 35°35′S | 4010 | 98 |
| | 9 de Julio (V) | 60°56′W; 35°30′S | 4315 | 71 |
| | Ameghino (V) | 62°24′W; 34°52′S | 1840 | 68 |
| | Hipólito Yrigoyen (V) | 62°23′W; 34°55′S | 1650 | 76 |
| | Trenque Lauquen (V) | 62°39′W; 36°03′S | 5530 | 78 |
| Northern Hills | Azul (A, V) | 59°53′W; 37°02′S | 6707 | 44 |
| | Tandil (A, V) | 59°14′W; 37°18′S | 5015 | 50 |
| | Olavarría (A, V) | 60°37′W; 36°51′S | 7940 | 48 |
| | Balcarce (A, V) | 58°25′W; 37°43′S | 4200 | 48 |
| | Benito Juárez (V) | 59°51′W; 37°10′S | 5490 | 56 |
| Semi-arid Plains | Trenel (A, V) | 64°10′W; 35°34′S | 1554 | 73 |
| | Capital (A, V) | 64°08′W; 36°30′S | 1775 | 92 |
| | Atreucó (A, V) | 63°45′W; 37°03′S | 3420 | 55 |
| | Catriló (A, V) | 63°39′W; 36°36′S | 2248 | 93 |
| | Realicó (A, V) | 64°11′W; 35°12′S | 1920 | 95 |
| | Conelo (V) | 64°30′W; 36°02′S | 6170 | 35 |

## 4. Results and discussion

### 4.1. Relationship between TVDI, solar radiation and yield

Fig. 3 shows the relationship between TVDI, TVDI-solar radiation and wheat yield in Northern Hills and Semi-arid Plains. After the TVDI-Rs-yield comparison analysis, it was found that November-December and October-November were the critical months for Northern Hills and Semi-arid Plains, respectively. Harvest usually occurs in December-January. Regarding the response of yield to TVDI, results are consistent with the previous work shown in Holzman et al. (2014a,b), where a generalized model was discussed. In both areas a quadratic function represents the yield variability, reflecting that yield decreases due to water deficit and excess with maximum yield for intermediate cumulative TVDI (≈0.8 in Northern Hills and 1.2 in Semi-arid Plains). It should be noted that yield losses due to water excess (minimum and stable TVDI values would indicate water excess in flat lands as in the Argentine Pampas) are more important in Northern Hills (humid region) with values about 75% with respect to the maximum yield. Adjustment for Semi-arid Plains shows the low productivity of the region mainly due to poorer soils (pedogenetic development and organic matter content), lower technology adoption and fertilization. On the other hand, although yield estimation through vegetation indices has been extensively analyzed, the TVDI model shows better performance than works which analyze only vegetation indices (Johnson, 2016; Mkhabela et al., 2011; Moriondo et al., 2007; Wall et al., 2008), reflecting that the combination with LST provides information about surface energy balance and improves the results.

In Northern Hills, the incorporation of solar radiation data improves the coefficient of determination (Fig. 3a). The validation results (Table 3) in this region were better than those obtained with TVDI. Also, in USA and Europe (Wu et al., 2014) showed the potential of a simple greenness and radiation model, driven by EVI, LST and global coarse resolution radiation data, to predict 8-day gross primary production in cultivated areas. The critical growth stage of wheat in humid and sub-humid areas of the Argentine Pampas covers months with occasional soil water excess, given that during winter extensive areas are represented by bare soil and mainly fallow (especially under direct seeding and periods between summer crops har-

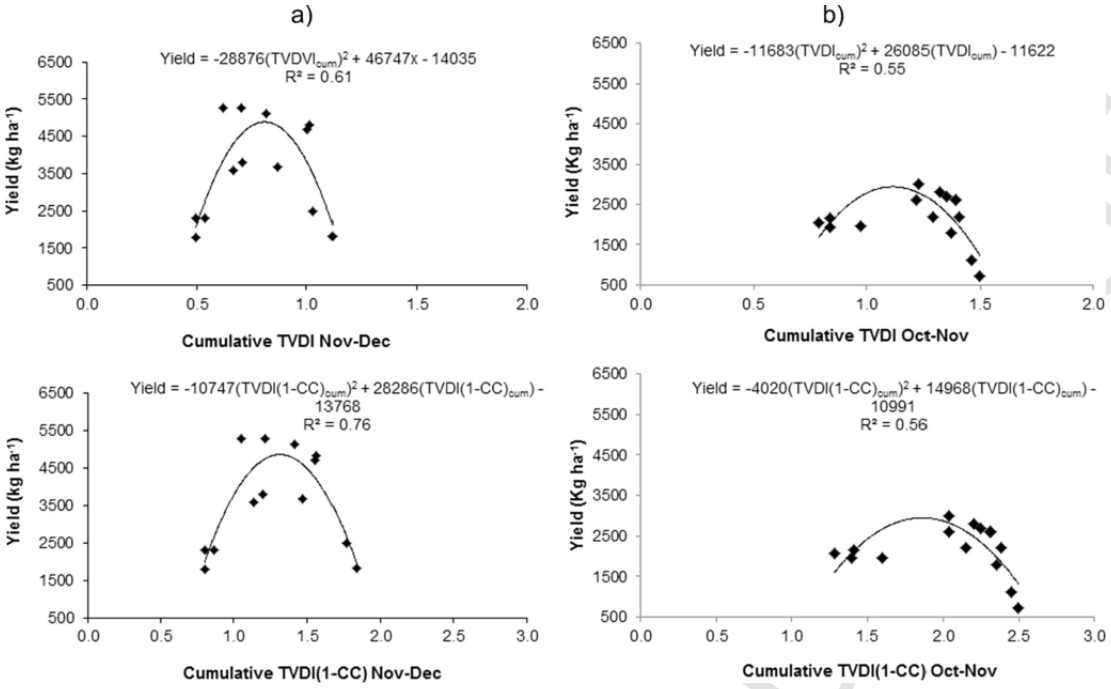


**Fig. 3.** Adjustment models of wheat yield as a function of TVDI and TVDI-solar radiation in (a) Northern Hills, (b) Semi-arid Plains.

**Table 3**
Validation parameters of models using TVDI and TVDI-solar radiation data for the four analyzed regions.

| Crop | Agro-climatic region | Validation parameters | TVDI | TVDI (1-CC) |
|---|---|---|---|---|
| Wheat | Northern Hills | n | 10 | |
| | | RMSE | 650 | 330 |
| | | RE | 0.17 | 0.15 |
| | | d | 0.72 | 0.81 |
| | Semi-arid Plains | n | 15 | |
| | | RMSE | 425 | 440 |
| | | RE | 0.21 | 0.22 |
| | | d | 0.88 | 0.85 |
| Soybean | Sandy Pampas | n | 21 | |
| | | RMSE | 460 | 825 |
| | | RE | 0.16 | 0.28 |
| | | d | 0.79 | 0.37 |
| | Endorreic Pampas | n | 17 | |
| | | RMSE | 420 | 430 |
| | | RE | 0.15 | 0.15 |
| | | d | 0.79 | 0.73 |
| Corn | Sandy Pampas and Endorreic Pampas | n | 48 | |
| | | RMSE | 1010 | 1000 |
| | | RE | 0.13 | 0.13 |
| | | d | 0.80 | 0.81 |
| | Northern Hills | n | 10 | |
| | | RMSE | 880 | 990 |
| | | RE | 0.14 | 0.16 |
| | | d | 0.84 | 0.79 |
| | Semi-arid Plains | n | 14 | |
| | | RMSE | 620 | 1300 |
| | | RE | 0.16 | 0.34 |
| | | d | 0.67 | 0.44 |

vest and winter crops sowing). Thus, soil water losses come mainly from surface soil evaporation. The low atmospheric evaporative demand, mainly explained by reduced incoming solar radiation, favors infiltration and then water excess. Conversely, in Semi-arid region the incorporation of the radiative factor did not produce improvements (Fig. 3b and Table 3). In this region the most important limiting variable is taken into account through the soil moisture factor, which reflects different processes such as low soil water retention, high atmospheric evaporative demand and highly variable rainfall.

These results are in agreement with (Lollato and Edwards, 2015) about that precipitation during critical stage would be the most important regulator of wheat yield and solar radiation a fine controller of yield in dryland. Lollato et al. (2017) reported that cumulative precipitation accounted for the largest proportion of variation in rainfed wheat in U.S southern Great Plains. They found that water supply becomes an important determinant of dryland wheat yield in the west and west-central regions. Water scarcity and high temperature can accelerate wheat senescence and decrease grain yield (Asseng et al., 2011). Also, Barkley et al. (2014) proposed that rainfall distribution is often the most limiting factor for wheat productivity in Kansas. Conversely, Lollato et al. (2017) noted that in the east region, characterized by greater cumulative precipitation, solar radiation becomes a stronger determinant of grain yield. In such cases, their results indicated a positive effect of solar radiation. Our results showed that daily average Rs (2001–2015) varied between 231 and 328 w m$^{-2}$ day$^{-1}$, with minimum values during October and February in Northern Hills and maximum values during December in Semi-arid Plains (considering only October-February). The joint effect of water excess and Rs could explain the yield loss in Northern Hills in humid periods. The amount of absorbed solar radiation determines the amount of energy available for crop growth, but also water excess can limit the canopy development and hence, the intercepted solar radiation. Indeed, Menéndez and Satorre (2007) pointed out that future hypothetical scenarios involving radiation reduction suggest that grain number would be the most affected component of wheat grain yield in the Argentine Pampas.

The adjustments between soil moisture, radiative factors and soybean yield in Sandy and Endorreic Pampas are shown in Fig. 4. January-February were found as the critical months and usually harvest date is March-April. In both regions the TVDI and yield are strongly correlated with linear adjustments and $R^2$ values consistent with previous works that analyze LST, NDVI, rainfall estimates or crop water stress indices (Holzman et al., 2014a; Marti et al., 2007; Mkhabela et

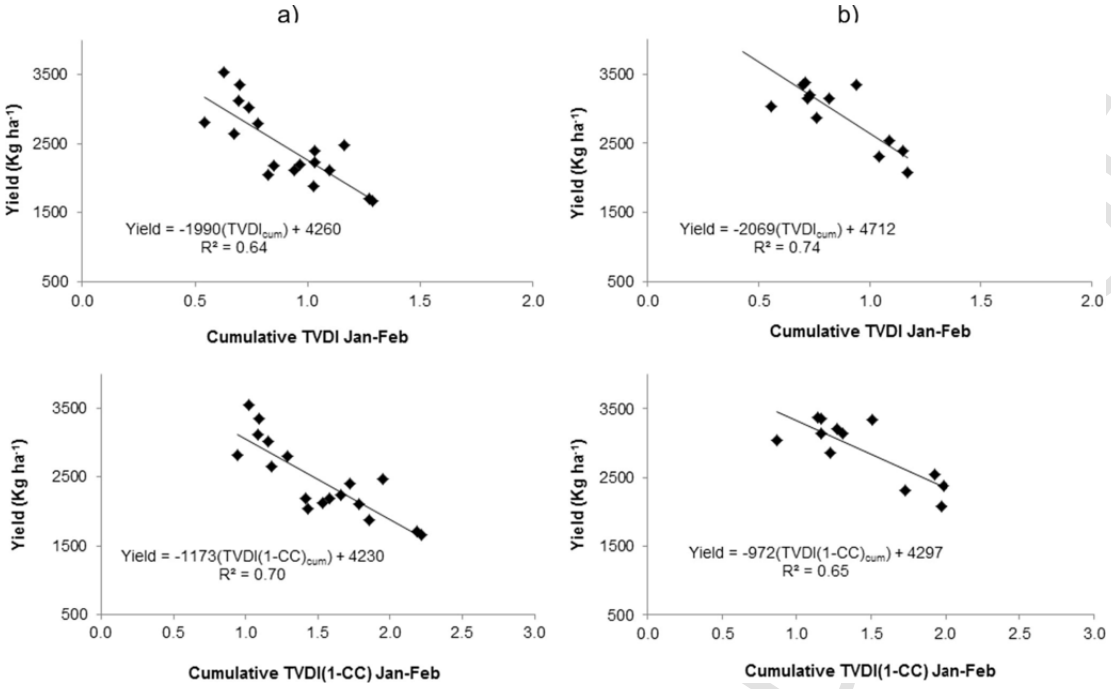


**Fig. 4.** Adjustment models of soybean yield as a function of TVDI and TVDI-solar radiation in (a) Sandy Pampas, (b) Endorreic Pampas.

al., 2005; O'Shaughnessy et al., 2011; Rhee et al., 2010). The linear adjustments considering TVDI were similar in both regions, showing that yield losses at regional scale are mainly explained by soil water deficit. Although the inclusion of the radiative factor increased slightly the $R^2$ in Sandy Pampas (Fig. 4a), the validation parameters (Table 3) show a poorer performance than the one obtained by TVDI model. These results suggest that soil moisture is the decisive factor determining soybean yield in these regions. These findings are consistent with (Johnson, 2014), that reported positive and negative correlation between soybean yield and MODIS NDVI (250 m) and daytime LST (1 km), respectively (correlation coefficient between 0.5 and 0.7). Also, in Brazil Gusso et al. (2014) found high correlation ($R^2 = 0.82$) between canopy LST during grain filling and soybean yield.

On the other hand, Xin et al. (2016) reported a non-linear response of leaf photosynthesis of soybean and corn to absorption of direct and diffuse radiation. They proposed that during clear days, the photosynthetic rates of sunlit leaves are often near light saturation due to direct beam components. On cloudy days, the photosynthetic rates of canopy leaves are near linearly related to radiation absorption. They measured light use efficiency 1.50 and 1.70 times higher during cloudy days than clear-sky days. Although they conclude that differences between these conditions are almost insignificant on an 8-day basis, the cumulative process could contribute to compensate lower incoming radiation. This may explain the low influence of radiation attenuation in Sandy and Endorreic Pampas on yield. This point needs further detailed analyses for the study area.

Fig. 5 shows the adjustments between TVDI, solar radiation and corn yield in three study regions. Considering the similarity between adjustments for Sandy and Endorreic Pampas, these regions were jointly analyzed. In both regions, January and February were the critical months for corn yield (Fig. 5a). About soil moisture, the linear adjustment indicates that water deficit is the regional limiting factor causing yield losses up to 60% (2007–2008 campaign) in relation to the maximum yield. Adjustment and validation parameters indicate that the inclusion of radiative factor does not produce significant improvements of the model, with an estimation error about 13% in relation to the average yield (Table 3). These results are comparable with the ones reported in Holzman and Rivas (2016) using TVDI. In Northern Hills and Semi-arid Plains, the critical month was December. Differences are noticeable in relation to the lower production capacity in the semi-arid area (4500 kg ha$^{-1}$ vs 8000 kg ha$^{-1}$) and higher TVDI values (0.85 vs 0.61) (Fig. 5b and c). Linear adjustment indicates that water deficit is crucial in the semi-arid region. The quadratic model shows that, although corn is a summer crop, the effect of water excess is noticeable in Northern Hills producing around 40% of yield loss with respect to optimum values.

In Northern Hills, the radiative factor produces improvements ($R^2 = 0.82$) in relation to the use of TVDI alone ($R^2 = 0.72$) (Fig. 5b). However, validation parameters do not show the advantage of using solar radiation data in this region. These results may indicate that limitation for corn yield during humid campaigns (2002–2003) is due to water excess rather than due to reduction of incoming solar radiation. In this region, the source of root zone soil moisture excess in spring-early summer months is frequently explained by shallow groundwater level (1m depth during early December 2002, 36°46′00.44″S; 59°52′51.57″W) (Varni et al., 1999). In this sense, previous works have shown that shallow water table can significantly reduce corn yield (Kanwar et al., 1988). Shrestha et al. (2017) found important effects of flood on corn yield in the major corn production region of US, with linear relation between the NDVI and yield. Other works explained the processes related to water excess and corn yield loss: inhibition of plants to retain nutrition required for its development, reduction of total root volume and air exchange between soil and atmosphere, less transport of water and nutrients through the roots to the shoot (Sakamoto et al., 2011; Wesseling, 1974). In Semi-arid Plains, the inclusion of the radiative factor deteriorates the results (Fig. 5c and Table 3), indicating that the incorporation of root zone soil moisture deficit provides good results, even in comparison with more complex approaches based on remotely sensed data (Ines et al., 2013; Xin et al., 2013). Also, the Rs was more uniform in Semi-arid Plains than in the other analyzed regions, being less useful for yield estimation. The lower performance of the model in Semi-arid Plains may be explained by the effect of subpixel heterogeneity, given the

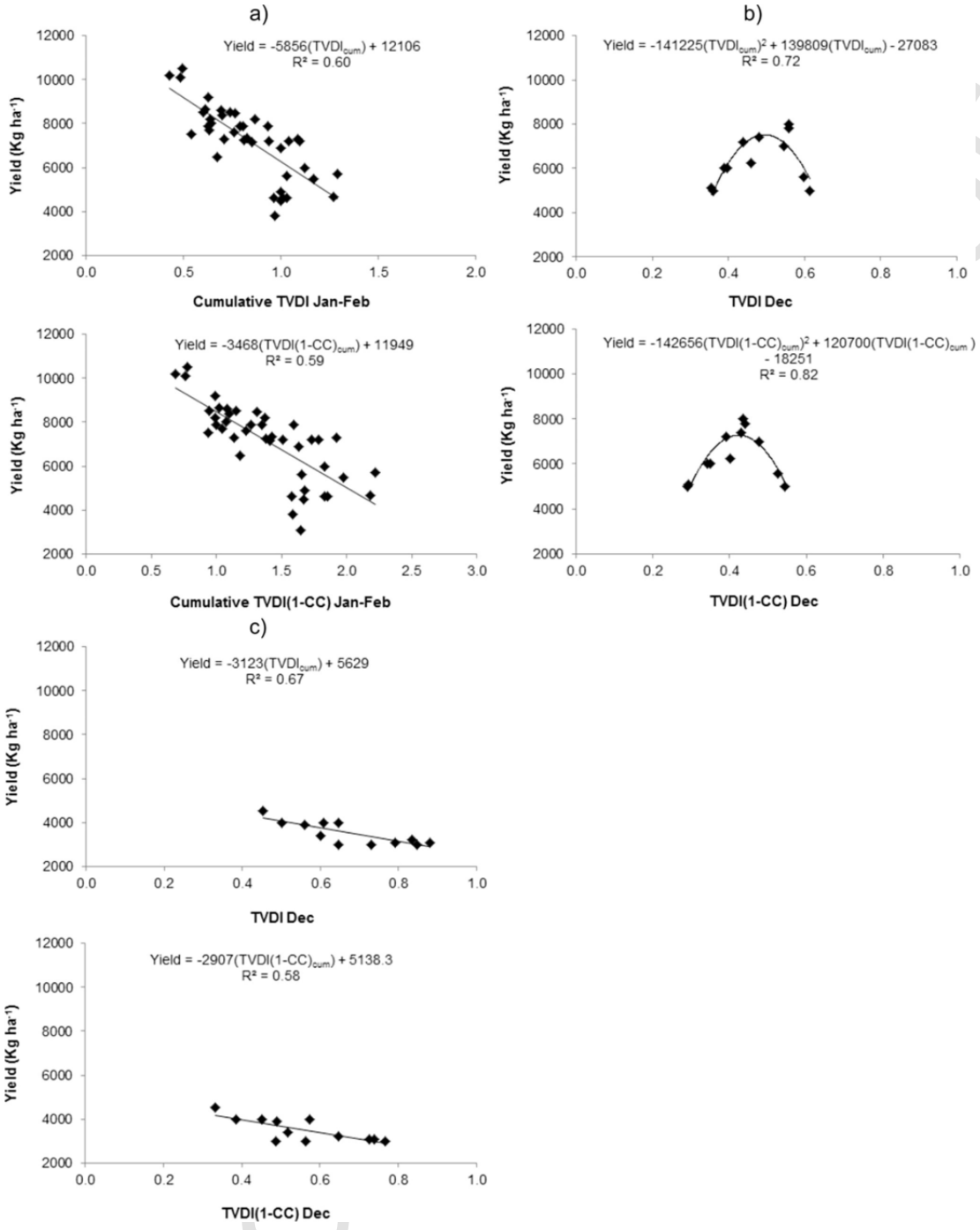


**Fig. 5.** Adjustment models of corn yield as a function of TVDI and TVDI-solar radiation in (a) Sandy Pampas and Endorreic Pampas, (b) Northern Hills, (c) Semi-arid Plains.

sparse cultivated fields and the coexistence of different crops (Atzberger and Rembold, 2013). Finally, considering that harvest usually occurs in late-February in Semi-arid Plains and late-March in Northern Hills, the model gives corn yield estimates 2–3 months prior to harvest.

According to the adjustments obtained in the study area, a general model depending on soil moisture and incoming solar radiation can be discussed (Fig. 6). This model can be proposed as a quadratic approach with three domains:

– A: is defined by optimum soil moisture and incoming solar radiation conditions. Crops are grown under non-limiting conditions, including no limited soil water (the actual evapotranspiration meeting crops requirements) and solar radiation (the rate of photosynthesis is close to the photosynthetic capacity), and all biotic stresses properly managed (Van Ittersum et al., 2013). For example, for wheat crop in humid region as Northern Hills, monthly CC values around 13–23% and TVDI 0.30–0.45 during critical stage are representative of this domain. According to a validation of TVDI carried out in Northern Hills, these values correspond to ap-

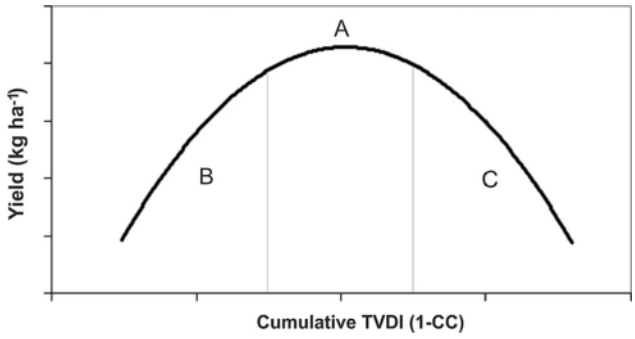


**Fig. 6.** General model for yield estimation based on TVDI and incoming solar radiation.

proximately 18–25% relative soil moisture at 40 cm depth (Holzman et al., 2014a,b). In Semi-arid Plains, these values are: CC ≈ 12–20% and TVDI ≈ 0.55–0.65. It should be noted that these values are indicative, given that the final yield will be a combination of SM and radiative factors. This is in agreement with (Lollato et al., 2017), who found in U.S. Great Plains that the highest rainfed wheat yield was achieved with abundant cumulative solar radiation and precipitation and intermediate/cool temperature. This effect allows extend crop cycle and grain filling periods. It should be noted that optimum yield can be variable depending on different factors such as genotype improvement, technological development, fertilization and irrigation.

- B: yield loss increases mainly due to water excess and, secondly, owing to incoming solar radiation shortage. This can be especially expected in humid areas and winter crops. In these environments, waterlogging during wetter years can be a reason of yield loss. Also, a reduced drainage due to dense subsoils (e.g. Bt horizon) can produce agricultural chemicals accumulation and generate algal blooms and other toxicities (Passioura, 2006). However, it should be noted the joint effect of soil moisture and solar radiation, given that water excess limits the canopy development and hence, the intercepted solar radiation. Passioura (2006) suggested that solar radiation is an important limiting factor for wheat yield when cumulative seasonal precipitation is higher than 500 mm, as in the case of humid region in our study area.
- C: yield loss is mainly explained by soil water deficit. This is expected in soils with low water retention capacity (e.g. sandy soils) and summer crops. Under these conditions, crops may fail to fill their grain adequately because of the low soil water content. They may be exposed to the heat and aridity of late spring and summer (Richards, 1991). Passioura (2006) reported that water deficits during critical stages can severely damage seed set through pollen sterility or premature end grain filling. This author stated that water deficits in maize can lead to lack of fertilization. In semi-arid and arid environments, water lost by direct evaporation from the soil can be important, especially during early stages of vegetative phases, decreasing water availability for subsequent phases (e.g. critical growth stages). Also, these environments are usually characterized by highly variable rainfall. A preponderance of small falls of rain can lead to large water losses by direct evaporation from the soil. Conversely, heavy rain events can favor losses of water by runoff. In sandy soils, water losses by soil evaporation and drainage beyond the crop roots reach can be important. This process is expected to be more noticeable in cases of soils with physical limitations to deep root development (e.g. saline, sodic or dense subsoils). In addition, water stress (and hence high canopy temperature) frequently depresses yield by causing accelerated crop development with the consequent shorter season and less cumulative radiation interception. In this case, crop yield could be mainly explained by TVDI during the critical growth stage. For example, a typical condition is represented by TVDI ≥ 0.65 (wheat and corn) and TVDI ≥ 0.55 (soybean and corn), for Semi-arid Plains and Sandy Pampas, respectively. The latter value corresponds to a soil moisture content lower than 12% at 60 cm depth (Holzman et al., 2014b).

### *4.2. Estimating spatial crop yield variability*

Based on TVDI and radiation model, maps of expected wheat and soybean yield are presented as an example for Northern Hills and Endorreic Pampas, respectively (Fig. 7). We assumed that cultivated areas are represented by wheat and soybean, respectively, given that in the study area masks of crop type are not currently available. On the other hand, the CERES product was resampled to match up with the 1 km resolution of TVDI. Large spatial yield variability is noticeable in both regions, with maximum yield coexisting next to minimum yield. In Northern Hills, maximum yields are observed in most of the area during normal periods (Fig. 7c). During the dry period, highest yields are located on the southeast probably due to the oceanic influence (Fig. 7e). In Endorreic Pampas the model reflects an east–west gradient consistent with rainfall and soil quality decreases westward. Also, in this region maximum soybean yields are predominant in normal period (Fig. 7d). It should be noted that CERES product has 1 degree spatial resolution and incoming solar radiation is not as variable as soil moisture. In this sense, the high yield spatial variability is mainly explained by TVDI, which reflects depressions, soils with limited water content and areas with vigorous vegetation cover where evapotranspiration is high (Holzman et al., 2014a).

## 5. Conclusions

Argentina produces the 18% of global soybean production (≈53 million tonnes per year) and is the thirteenth wheat producer (≈14 millon tonnes per year). In addition, the Argentine Pampas is the most productive region in Argentina (≈90% of total production). In this work, a model based on remotely sensed incoming solar radiation and proxy of root zone soil moisture to forecast wheat, soybean and corn yield was evaluated in Argentine Pampas. This approach represents a simplification of the functioning of soil-vegetation atmosphere system and crop productivity according to water and energy availability. TVDI from MODIS/Aqua EVI and LST was calculated as a soil moisture proxy in the study area. Solar radiation data were obtained from CERES product. Results indicate that solar radiation data is a significant variable for yield estimation in humid regions and winter crops. In this case, the combination of the two variables provides improved results in comparison with the model based solely on TVDI. On the other hand, crop water stress is essential in semi-arid areas and summer crops, providing good results (RMSE = 400–1000 kg ha$^{-1}$, depending on crop and region) and simplifying the method.

Although meteorological data are not required for TVDI calculation, its parameters should be adequately defined at large region level with uniform atmospheric forcing. Also, the specific parameters of TVDI-radiation-yield adjustments shown may vary in other regions, depending on the prevalence of water deficit or excess. However, after a calibration process using reliable crop yield dataset, the general TVDI-solar radiation proposed model can be spatially applicable in other productive regions in the world (e.g. Ukraine, USA, Canada). In case of poor ground data availability for calibration, the proposed general model can be used to evaluate conditions of optimum productivity and yield losses at regional/landscape scales as a part of a drought/water excess monitoring system. In addition, information

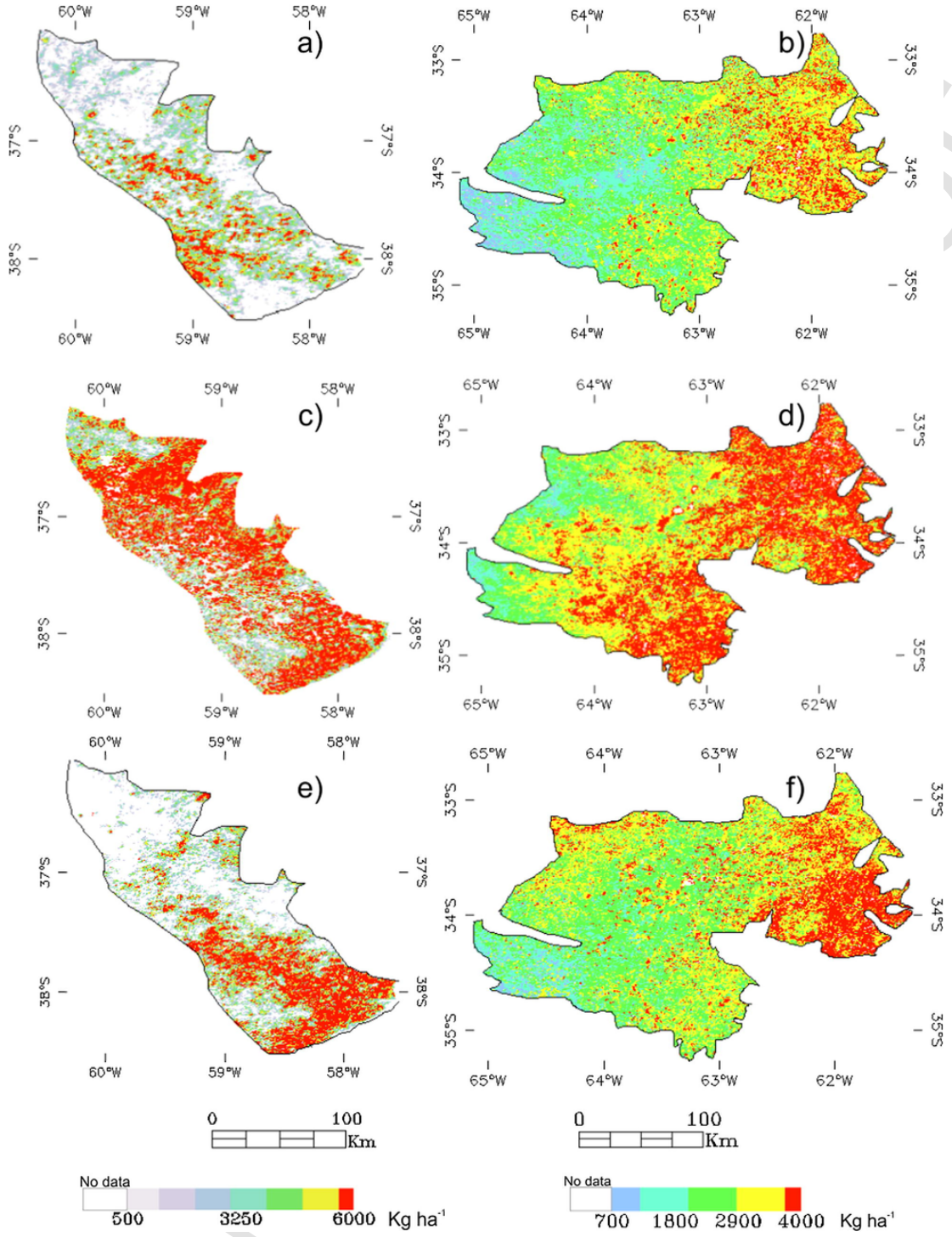


**Fig. 7.** Maps of estimated yield based on the TVDI-solar radiation model. Wheat in Northern Hills: (a) humid (2002–2003), (c) normal (2009–2010), (e) dry (2007–2008) periods. Soybean in Endorreic Pampas: (b) humid (2002–2003), (d) normal (2009–2010), (f) dry (2007–2008) periods. White areas indicate no data due to cloud cover, water bodies or values out of analyzed range.

about interannual variability of planting dates should be needed in other regions to determine the critical growth stages of crops.

The results obtained are promising at regional scales, although future studies can test the model at finer resolution (e.g. 250 m). In this sense, the sub-pixel heterogeneity could be a reason of the lower performance in the semi-arid region with sparse cultivated areas and different crops. Also, crop types mask can improve the results and less important crops could be analyzed. Nevertheless, the approach showed good performance in Argentine Pampas (RE≤13%), allowing crop estimation 1–3 months prior to harvest. Moreover, the results obtained are comparable with those obtained by more complex methods based on remotely sensed data, which suggest the potential of this approach as an early indicator of expected yield. Thus, the proposed method can be useful for decision makers. Finally, this work is in

agreement with global trends about crop yield estimation using easy accessible data and products.

## Acknowledgements

This work was supported by CONICET (Consejo Nacional de Investigaciones Científicas y Técnicas) and IHLLA (Instituto de Hidrología de Llanuras "Dr. Eduardo J. Usunoff"). The authors also would like to thank CIC (Comisión de Investigaciones Científicas de Buenos Aires), UNCPBA (Universidad Nacional del Centro de la provincia de Buenos Aires) and reviewers that have helped us to improve the manuscript.

## References

Alexandratos, N., Bruinsma, J., 2012. World Agriculture Towards 2030/2050: The 2012 Revision. ESA Working Paper No 12-30. Rome.

Anderson, M.C., Zolin, C.A., Sentelhas, P.C., Hain, C.R., Semmens, K., Yilmaz, M.T., Gao, F., Otkin, J.A., Tetrault, R., 2016. The evaporative stress index as an indicator of agricultural drought in Brazil: an assessment based on crop yield impacts. Rem. Sens. Environ. 174, 82–99. https://doi.org/10.1016/j.rse.2015.11.034.

Arino, O., Bicheron, P., Achard, F., Latham, J., Witt, R., Weber, J.-L., 2008. GlobCover: the most detailed portrait of Earth. ESA Bull. 136, 24–31.

Asseng, S., Foster, I., Turner, N.C., 2011. The impact of temperature variability on wheat yields. Global Change Biol. 17, 997–1012.

Atzberger, C., Rembold, F., 2013. Mapping the spatial distribution of winter crops at sub-pixel level using AVHRR NDVI time series and neural nets. Rem. Sens. 5, 1335–1354.

Barkley, A., Tack, J., Nalley, L.L., Bergtold, J., Bowden, R., Fritz, A., 2014. Weather, disease and wheat breeding effects on Kansas wheat varietal yields 1985–2011. Agron. J. 106, 227–235.

Bhattacharya, B.K., Mallick, K., Nigam, R., Dakore, K., Shekh, A.M., 2011. Efficiency based wheat yield prediction in a semi-arid climate using surface energy budgeting with satellite observations. Agric. For. Meteorol. 151, 1394–1408.

Carmona, F., Orte, P.F., Rivas, R., Wolfram, E., Kruse, E., 2017. Development and analysis of a new solar radiation atlas for Argentina from ground-based measurements and CERES_SYN1deg data. Egypt. J. Rem. Sens. Space Sci.(in press).

Carmona, F., Rivas, R., Caselles, V., 2014. Estimation of daytime downward longwave radiation under clear and cloudy skies conditions over a sub-humid region. Theor. Appl. Climatol. 115, 281–295.

Farquhar, G.D., Sharkey, T.D., 1982. Stomatal conductance and photosynthesis. Annu. Rev. Plant Physiol. 33, 317–345.

Global Harvest Initiative, 2014. 2014 Global Agricultural Productivity Report.

Gusso, A., Ducati, J.R., Veronez, M.R., Sommer, V., da Silveira Junior, L.G., 2014. Monitoring heat waves and their impacts on summer crop development in Southern Brazil. Agric. Sci. 5, 353–364. https://doi.org/10.4236/as.2014.54037.

Holzapfel, C.B., Lafond, G.P., Brandt, S.A., Bullock, P.R., Irvine, R.B., Morrison, M.J., May, W.E., James, D.C., 2009. Estimating canola (Brassica napus L.) yield potential using an active optical sensor. Can. J. Plant Sci. 89, 1149–1160.

Holzman, M., Rivas, R., Bayala, M., 2014. Subsurface soil moisture estimation by VI–LST method. IEEE Geosci. Rem. Sens. Lett. 11, 1951–1955. https://doi.org/10.1109/LGRS.2014.2314617.

Holzman, M., Rivas, R., Carmona, F., 2017. A method for soil moisture probes calibration and validation of satellite estimates. MethodsX 4, 243–249. https://doi.org/10.1016/j.mex.2017.07.004.

Holzman, M.E., Rivas, R., Piccolo, M.C., 2014. Estimating soil moisture and the relationship with crop yield using surface temperature and vegetation index. Int. J. Appl. Earth Obs. Geoinf. 28, 181–192. https://doi.org/10.1016/j.jag.2013.12.006.

Holzman, M.E., Rivas, R.E., 2016. Early maize yield forecasting from remotely sensed temperature/vegetation index measuremnts. IEEE J. Sel. Top. Appl. Earth Obs. Rem. Sens. 9, 507–519. https://doi.org/10.1109/JSTARS.2015.2504262.

Ines, A.V.M., Das, N.N., Hansen, J.W., Njoku, E.G., 2013. Assimilation of remotely sensed soil moisture and vegetation with a crop simulation model for maize yield prediction. Rem. Sens. Environ. 138, 149–164.

Kanwar, R.S., Baker, J.L., Mukhtar, S., 1988. Excessive soil water effects at various stages of development on the growth and yield of corn. Agric. Biosyst. Eng. Pub. 31 (1), 133–141.

Kurc, S.A., Small, E.E., 2004. Dynamics of evapotranspiration in semiarid grassland and shrubland ecosystems during the summer monsoon season, central New Mexico. Water Resour. Res. 40, 1–15.

Johnson, D.M., 2016. A comprehensive assessment of the correlations between field crop yields and commonly used MODIS products. Int. J. Appl. Earth Obs. Geoinf. 52, 65–81. https://doi.org/10.1016/j.jag.2016.05.010.

Johnson, D.M., 2014. An assessment of pre- and within-season remotely sensed variables for forecasting corn and soybean yields in the United States. Rem. Sens. Environ. 141, 116–128.

Leroux, L., Baron, C., Zoungrana, B., Traoré, S.B., Seen, D.Lo, Bégué, A., 2016. Crop monitoring using vegetation and thermal indices for yield estimates: case study of a rainfed cereal in semi-arid West Africa. IEEE J. Sel. Top. Appl. Earth Obs. Rem. Sens. 9, 347–362.

Liu, L., Liao, J., Chen, X., Zhou, G., Su, Y., Xiang, Z., Wang, Z., Liu, X., Li, Y., Wu, J., Xiong, X., Shao, H., 2017. The Microwave temperature vegetation drought index (MTVDI) based on AMSR – E brightness temperatures for long-term drought assessment across China (2003–2010). Rem. Sens. Environ. 199, 302–320. https://doi.org/10.1016/j.rse.2017.07.012.

Lollato, R.P., Edwards, J.T., 2015. Maximum attainable winter wheat yield and resource use efficiency in the southern Great Plains. Crop Sci. 55, 2863–2876.

Lollato, R.P., Edwards, J.F., Ochsner, T.E., 2017. Meteorological limits to winter wheat productivity in the U.S. Southern Great Plains. Field Crops Res. 203, 212–226.

Mallick, K., Bhattacharya, B.K., Patel, N.K., 2009. Estimating volumetric surface moisture content for cropped soils using a soil wetness index based on surface temperature and NDVI. Agric. For. Meteorol. 149, 1327–1342.

Marti, J., Bort, J., Slafer, G.a., Araus, J.L., 2007. Can wheat yield be assessed by early measurements of Normalized Difference Vegetation Index?. Ann. Appl. Biol. 150, 253–257. https://doi.org/10.1111/j.1744-7348.2007.00126.x.

Menéndez, F.J., Satorre, E.H., 2007. Evaluating wheat yield potential determination in the Argentine Pampas. Agric. Syst. 95, 1–10.

Mkhabela, M.S., Mkhabela, M.S., Mashinini, N.N., 2005. Early maize yield forecasting in the four agro-ecological regions of Swaziland using NDVI data derived from NOAA's-AVHRR. Agric. For. Meteorol. 129, 1–9.

Mkhabela, Bullock, P., Raj, S., Wang, S., Yang, Y., 2011. Crop yield forecasting on the Canadian Prairies using MODIS NDVI data. Agric. For. Meteorol. 151, 385–393.

Mladenova, I.E., Bolten, J.D., Crow, W.T., Anderson, M.C., Hain, C.R., Johnson, D.M., Mueller, R., 2017. Intercomparison of soil moisture, evaporative stress, and vegetation indices for estimating corn and soybean yields over the U.S. IEEE J. Sel. Top. Appl. Earth Obs. Rem. Sens. 10, 1328–1343.

Monteith, J.L., 1977. Climate and efficiency of crop production in Britain. Phil. Trans. Roy. Soc. Lond. Ser. B – Biol. Sci. 281, 277–294.

Moriondo, M., Maselli, F., Bindi, M., 2007. A simple model of regional wheat yield based on NDVI data. Eur. J. Agron. 26, 266–274.

Nemani, R., Running, S., 1997. Land cover characterization using multi-temporal red, near-IR and thermal-IR data from NOAA/AVHRR. Ecol. Appl. 7 (1), 79–90.

Nutini, F., Boschetti, M., Candiani, G., Bocchi, S., Brivio, P., 2014. Evaporative fraction as an indicator of moisture condition and water stress status in semi-arid rangeland ecosystems. Rem. Sens. 6 (7), 6300–6323.

O'Shaughnessy, S.A., Evett, S.R., Colaizzi, P.D., Howell, T., 2011. Using radiation thermography and thermometry to evaluate crop water stress in soybean and cotton. Agric. Water Manage. 98, 1523–1535.

Oficina de Riesgo Agropecuario-MAGyP-Argentina [WWW Document], 2017. URL http://www.ora.gov.ar/ (accessed 5.4.17).

Passioura, J., 2006. Increasing crop productivity when water is scarce—from breeding to field management. Agric. Water Manage. 80, 176–196.

Rhee, J., Im, J., Carbone, G.J., 2010. Monitoring agricultural drought for arid and humid regions using multi-sensor remote sensing data. Rem. Sens. Environ. 114, 2875–2887. https://doi.org/10.1016/j.rse.2010.07.005.

Richards, R.A., 1991. Crop improvement for temperate Australia—future opportunities. Field Crops Res. 26, 141–169.

Rivas, R., Caselles, V., 2004. A simplified equation to estimate spatial reference evaporation from remote sensing-based surface temperature and local meteorological data. Rem. Sens. Environ. 93, 68–76.

Sakamoto, T., Wardlow, B.D., Gitelson, A.A., 2011. Detecting spatiotemporal changes of corn developmental stages in the U.S. corn belt using MODIS WDRVI Data. IEEE Trans. Geosci. Rem. Sens. 49, 1926–1936.

Sandholt, I., Rasmussen, K., Andersen, J., 2002. A simple interpretation of the suface temperature/vegetation index space for the assessment of surface moisture stress. Rem. Sens. Environ. 79, 213–224.

Sayago, S., Ovando, G., Bocco, M., 2017. Landsat images and crop model for evaluating water stress of rainfed soybean. Rem. Sens. Environ. 198, 30–39. https://doi.org/10.1016/j.rse.2017.05.008.

Shrestha, R., Di, L.P., Eugene, G., Yu, E.G., Kang, L.G., Shao, Y.Z., Bai, Y.Q., 2017. Regression model to estimate flood impact on corn yield using MODIS NDVI and USDA cropland data layer. J. Integr. Agric. 16, 398–407.

Smith, G., Priestley, K., Loeb, N., Wielicki, B., Charlock, T., Minnis, P., Doelling, D., Rutan, D., 2011. Clouds and earth radiant energy system (CERES), a review: past, present and future. Adv. Space Res. 48, 254–263.

Stisen, S., Sandholt, I., Nørgaard, A., Fensholt, R., Jensen, K.H., 2008. Combining the triangle method with thermal inertia to estimate regional evapotranspiration—applied to MSG-SEVIRI data in the Senegal River basin. Rem. Sens. Environ. 112, 1242–1255.

Tadesse, T., Senay, G.B., Berhan, G., Regassa, T., Beyene, S., 2015. Evaluating a satellite-based seasonal evapotranspiration product and identifying its relationship with other satellite-derived products and crop yield: a case study for Ethiopia. Int. J. Appl. Earth Obs. Geoinf. 40, 39–54. https://doi.org/10.1016/j.jag.2015.03.006.

Varni, M., Usunoff, E., Weinzettel, P., Rivas, R., 1999. Groundwater recharge in the Azul aquifer, Central Buenos Aires Province Argentina. Phys. Chem. Earth 24, 349–352.

Van Ittersum, M.K., Cassman, K.G., Grassini, P., Wolf, J., Tittonell, P., Hochman, Z., 2013. Yield gap analysis with local to global relevance-a review. Field Crops Res. 143, 4–17.

Wagle, P., Bhattarai, N., Gowda, P.H., Kakani, V.G., 2017. Performance of five surface energy balance models for estimating daily evapotranspiration in high biomass sorghum. ISPRS J. Photogramm. Rem. Sens. 128, 192–203. https://doi.org/10.1016/j.isprsjprs.2017.03.022.

Wall, L., Larocque, D., Léger, P., 2008. The early explanatory power of NDVI in crop yield modelling. Int. J. Rem. Sens. 29, 2211–2225.

Wesseling, J., 1974. Crop growth and wet soils. In: Van Schilfgaarde, J. (Ed.), Drainage for Agriculture. American Society of Agronomy, Madison, WI, pp. 7–37.

Willmot, C.J., 1981. On the validation of models. Phys. Geogr. 2, 184–194.

Wu, C., Gonsamo, A., Zhang, F., Chen, J.M., 2014. The potential of the greenness and radiation (GR) model to interpret 8-day gross primary production of vegetation. ISPRS J. Photogramm. Rem. Sens. 88, 69–79. https://doi.org/10.1016/j.isprsjprs.2013.10.015.

Xin, Q., Gong, P., Suyker, A.E., Si, Y., 2016. Effects of the partitioning of diffuse and direct solar radiation on satellite-based modeling of crop gross primary production. Int. J. Appl. Earth Obs. Geoinf. 50, 51–63. https://doi.org/10.1016/j.jag.2016.03.002.

Xin, Q., Gong, P., Yu, C., Yu, L., Broich, M., Suyker, A., Myneni, R., 2013. A production efficiency model-based method for satellite estimates of corn and soybean yields in the Midwestern US. Rem. Sens. 5, 5926–5943.